Computational Design of C_2-Symmetric Metallocene-Based Catalysts for the Synthesis of High Molecular Weight Polymers from Ethylene/Propylene Copolymerization

Tebikie Wondimagegn,[†] Dongqi Wang,[†] Abbas Razavi,[‡] and Tom Ziegler*,[†]

Department of Chemistry, University of Calgary, 2500 University Drive NW, Calgary, Alberta, Canada T2N 1N4 and Total Petrochemicals Research Feluy, Zone Industrielle C, B-7181 Seneffe (Feluy), Belgium

Received July 30, 2008

Indenyl-based C_2-symmetric metallocenes have been used extensively as catalysts for the synthesis of high molecular weight polymers from ethylene or propylene homopolymerization. However, the same catalysts afford only low molecular weight polymers in ethylene/propylene copolymerization. We have in a recent study shown [Wang et al. *Organometallics* **2008**, *27*, 2861] that the poor performance of fluorenyl-based C_1-symmetric zirconocenes in ethylene/propylene polymerization is a result of electronic effects. In the present computational study, we demonstrate how it is possible by substitutions in the 2- and 4-positions of the indenyl ligands to design catalysts that afford high molecular weight polymers from ethylene/propylene copolymerization.

Introduction

Olefin polymerization using single-site metallocenes is a subject of considerable importance in the polymer industry.[1−3] Extensive work has been carried out in the areas of regio- and stereospecificity. In addition, much emphasis has been given to molecular weight control for accessing economically viable polymeric materials. Single-site metallocenes have been exploited as catalysts for both homo- and copolymerization. Although these catalyst systems have shown promising results in homopolymerization, many problems have been encountered when two or more monomers are polymerized together. However, Naga,[4] Rieger,[5] Kaminsky,[6] Huang,[7] Coussens,[8] and co-workers have made important steps toward the development of efficient copolymerization catalysts.

In regio- and stereospecific single-site metallocene catalysis, steric control is achieved by modification of the metallocene structure. This prompted researchers to develop C_s-, C_2-, and C_1-symmetric catalysts by introducing appropriate substitutions on the metallocene rings. Figure 1 shows the different known C_s-, C_1, and C_2-symmetric catalysts. C_s-symmetric fluorenyl-containing metallocenes of the type (η^5-$C_5H_4CMe_2$-η^5−C_{13}-H_8)MCl_2 (M = Zr, Hf) were first reported by Razavi and co-workers (Figure 1a).[9,10] Following this report, C_1-symmetric catalysts (and their derivatives) have been developed with substituted variants of cyclopentadienyl (Cp), Figure 1b, and/or fluorenyl (Flu) groups (Figure 1c).[11,12] In these *ansa* complexes, the η^5-cyclopentadienyl and η^5-fluorenyl groups are bridged by an isopropylidene group. C_1-symmetric metallocene

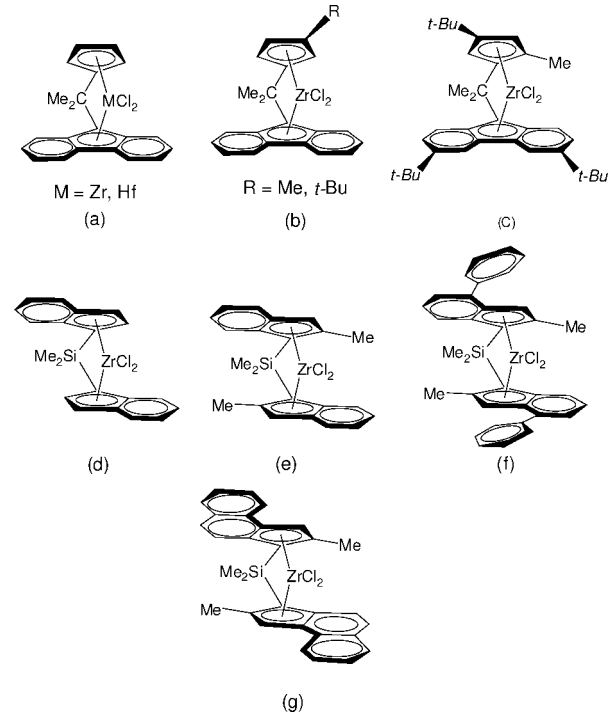

Figure 1. The different known C_s (a), C_1 (b, c) and C_2 (d−g) symmetric metallocenes.

* To whom correspondence should be addressed. E-mail: ziegler@ucalgary.ca.
† Department of Chemistry, University of Calgary.
‡ Total Petrochemicals Research Feluy, Zone Industrielle C.

(1) Alt, H. G.; Köppl, A. *Chem. Rev.* **2000**, *100*, 1205.
(2) Resconi, L.; Cavallo, L.; Fait, A.; Piemontesi, F. *Chem. Rev.* **2000**, *100*, 1253.
(3) Razavi, A.; Thewalt, U. *Coord. Chem. Rev.* **2006**, *250*, 155.
(4) Naga, N.; Ohbayashi, Y.; Mizunuma, K. *Macromol. Rapid Commun.* **1997**, *18*, 837–851.
(5) Voegele, J.; Troll, C.; Rieger, B. *Macromol. Chem. Phys.* **2002**, *203*, 1918.
(6) Seraidaris, T.; Lofgren, B.; Seppala, J. V.; Kaminsky, W. *Polymer* **2006**, *47*, 107.
(7) Yang, X.; Zhang, Y.; Huang, J. *Appl. Organometal. Chem.* **2006**, *20*, 130.
(8) Friederichs, N.; Wang, B.; Budzelaar, P. H. M.; Coussens, B. B. *J. Mol. Catal. A-Chem.* **2005**, *242*, 91.
(9) Ewen, J. A.; Jones, R. L.; Razavi, A.; Ferrara, J. D. *J. Am. Chem. Soc.* **1988**, *110*, 6255.
(10) Razavi, A.; Ferrara, J. *J. Organomet. Chem.* **1992**, *435*, 299.
(11) Miller, S. A.; Bercaw, J. E. *Organometallics* **2006**, *25*, 3576.
(12) Razavi, A.; Bellia, V.; Baekelmans, D.; Slawinsky, M.; Sirol, S.; Peters, L.; Thewalt, U. *Kinet. Catal.* **2006**, *47*, 257.

10.1021/om800731y CCC: $40.75 © 2008 American Chemical Society
Publication on Web 11/19/2008

catalysts are efficient in the production of isotactic polypropylene polymers with high molecular weights and melting point.[12] The C_2-symmetric catalysts produce isotactic polypropylene comparable in crystallinity with the polymer generated with conventional heterogeneous Ziegler−Natta catalysts (Figure 1f).[13] However, these C_2-symmetric catalysts show a severe decrease in molecular weight when used in copolymerization. Spaleck[13−15] (Figure 1f) and Brintzinger[16] (Figure 1g) have developed a catalyst which leads to a substantial increase in molecular weight by introducing 2-methyl and benzo substituents on silylene bridged bis(indenyl) zirconocenes. However, Rieger and co-workers[5] noted that the presence of a methyl substituent in position 2 of the indenyl ligand displays a significant decline of molecular weight of propylene-ethylene copolymers with an increase in ethylene monomer concentration (Figure 1e). In another study, for ethylene/propylene copolymerization, substituting Zr with Hf leads to an increase in molecular weight.[4]

In a recent computational study[17] on C_1-symmetric isotactic zirconocene catalyst, Figure 1c, we found that the substituents on the growing chain and olefin can modulate the activation barrier of β-hydrogen transfer which is the predominant mechanism for chain transfer. Therefore, a direct comparison of the barriers for β-hydrogen transfer ($\Delta H^{\ddagger}_{\beta H}$) and insertion ($\Delta H^{\ddagger}_{ins}$) can give us important clues about how to control molecular weight. In fact, an increase in $\Delta\Delta H^{\ddagger} = \Delta H^{\ddagger}_{\beta H} - \Delta H^{\ddagger}_{ins}$ will lead to an increase in the molecular weight. This difference ($\Delta\Delta H^{\ddagger}$) can be enhanced by suppressing β-hydrogen transfer to monomer. The β-hydrogen transfer to monomer pathway is effectively suppressed by introducing bulky substituents as we shall shortly see. This study does not examine the influence of substituents on regioselectivity, which may be an important factor for controlling molecular weight. Therefore, other factors including regioselectivity may be important contributors to the molecular weight trends observed experimentally for catalysts **1**−**3**.

The purpose of this investigation is to examine the electronic and steric (ligand substitution pattern) effects on C_2-symmetric, $B(C_6F_5)_3$-activated, $Me_2Si(2R_1\text{-}4R_2\text{-}Ind)_2ZrCl_2$ (R_1 = H, Me, *i*-Pr, *t*-Bu, Ph, tetrahydrofuran, cyclopentyl, cyclohexyl; R_2 = Ph, *t*-Bu; Ind = Indenyl) catalyst systems for isotactic polymerization (Figure 2). We shall discuss the possible interactions involving the growing chain, the monomer, and the substituents on the ligand. An understanding of these interactions shall guide us in improving the design of C_2-symmetric metallocenes for copolymerization. In order to gain insight into the relation between structural features and their performance, especially the resulting molecular weights in homo- and copolymerization, we have carried out a combined quantum mechanical and molecular mechanics (QM/MM) investigation on eleven catalytic systems (Figure 2). For each of the systems shown in Figure 2, we calculated first propylene attachment following propylene insertion (PP) to study the difference $\Delta\Delta H^{\ddagger}_{PP}$ between the activation energy of termination by β-hydrogen transfer to monomer and the activation energy of insertion. Here, $\Delta\Delta H^{\ddagger}_{PP}$ can provide information about molecular weight control in propylene homopolymerization. After that, we examined ethylene attachment following propylene insertion (EP) to study the difference $\Delta\Delta H^{\ddagger}_{EP}$ between the activation energy of termination by β-hydrogen transfer to monomer and the activation energy of insertion. Again, $\Delta\Delta H^{\ddagger}_{EP}$ is a measure for the molecular weight in ethylene/propylene copolymerization. For the ethylene/propylene copolymerization, the process of propylene attachment after ethylene insertion is not considered since a previous investigation[17] has shown that $\Delta\Delta H^{\ddagger}_{PE}$ is likely to be larger than $\Delta\Delta H^{\ddagger}_{EP}$ and thus not the crucial factor for the molecular weight in ethylene/propylene copolymerization.

Computational Details and Methods

Density functional theory calculations were carried out using the Amsterdam Density Functional (ADF) program system developed by Baerends et al.[18] and vectorized by Raveneck.[19] The numerical scheme applied was developed by te Velde et al.[20] and the geometry optimization procedure was based on the method of Verslius and Ziegler.[21] Slater-type double-ζ plus polarization basis sets were employed for H, B, C, O, F, Si, and Cl atoms, whereas triple-ζ plus polarization basis sets were used for the Zr atom. All of the calculations utilized the BP86 functional.[22] First-order scalar relativistic corrections were applied to the systems studied.[23−25]

Combined quantum-mechanical (QM) and molecular-mechanical (MM) models (QM/MM) have been applied throughout this study. In this model, the perfluorophenyl groups (C_6F_5) in the counterion, $[MeB(C_6F_5)_3]^-$, were replaced by MM atoms and Cl atoms were used to cap the QM system. The MM atoms were described using the SYBYL/TRIPOS 5.2 force field constants.[26] The code for QM/MM in ADF has been implemented by Woo et al.[27] The QM/MM model for $[MeB(C_6F_5)_3]^-$ has been validated in previous studies.[28] All of the calculations reported here have been carried out in the gas phase.

Results and Discussion

Catalyst Design Strategies. A strategy for designing efficient catalysts for isotactic homo- and copolymerizations has been developed based on steric and electronic considerations. Compounds **1**−**4** in Figure 2 are known catalysts in the literature

(13) Spaleck, W.; Kuber, F.; Winter, A.; Rohrmann, J.; Bachmann, B.; Antberg, M.; Dolle, V.; Paulus, E. F. *Organometallics* **1994**, *13*, 954.
(14) Spaleck, W.; Antberg, M.; Rohrmann, J.; Winter, A.; Bachmann, B.; Kiprof, B.; Behm, J.; Herrmann, W. A. *Angew. Chem.* **1992**, *104*, 1373.
(15) Spaleck, W.; Antberg, M.; Dolle, V.; Klein, R.; Rohrmann, J.; Winter, A. *New J. Chem.* **1990**, *14*, 499.
(16) Stehling, U.; Diebold, J.; Kirsten, R.; Roll, W.; Britzinger, H. H.; Jungling, S.; Mulhaupt, R.; langahuster, F. *Organometallics* **1994**, *13*, 965.
(17) Wang, D.; Toamsi, S.; Razavi, A.; Ziegler, T. *Organometallics* **2008**, *27*, 2861.
(18) (a) Baerends, E. J.; Ellis, D. E.; Ros, P. *Chem. Phys.* **1973**, *2*, 41. (b) Baerends, E. J.; Ros, P. *Chem. Phys.* **1973**, *2*, 52. (c) te Velde, G.; Baerends, E. J. *J. Comput. Phys.* **1992**, *92*, 84. (d) Fonseca, C. G.; Visser, O.; Snijders, J. G.; te Velde, G.; Baerends, E. J. In *Methods and Techniques in Computational Chemistry, METECC-95*; Clementi, E., Corongiu, G., Eds.; STEF: Cagliari, Italy, 1995; p 305.
(19) Ravenek, W. In *Algorithms and Applications on Vector and Parallel Computers*; te Riele, H. J. J., Dekker, T. J., van de Horst, H. A., Eds.; Elsevier: Amsterdam, 1987.
(20) (a) te Velde, G.; Baerends, E. J. *J. Comput. Chem.* **1992**, *99*, 84. (b) Boerrigter, P. M.; te Velde, G.; Baerends, E. J. *Int. J. Quantum Chem.* **1998**, *33*, 87.
(21) Verslius, L.; Ziegler, T. *J. Chem. Phys.* **1988**, *88*, 322.
(22) (a) Becke, A. D. *Phys. Rev. A* **1988**, *38*, 3098. (b) Perdew, J. P. *Phys. Rev. B* **1986**, *33*, 8822 Erratum. (c) Perdew, J. P. *Phys. Rev. B* **1986**, *34*, 7406.
(23) Snijders, J. G.; Baerends, E. J.; Ros, P. *Mol. Phys.* **1979**, *38*, 1909.
(24) Boerrigter, P. M.; Baerends, E. J.; Snijders, J. G. *Chem. Phys.* **1988**, *122*, 357.
(25) Ziegler, T.; Tschinke, V.; Baerends, E. J.; Snijders, J. G.; Ravenek, W. *J. Phys. Chem.* **1989**, *93*, 3050.
(26) Clark, M.; Cramer, R. D. I.; van Opdenbosch, N. *J. Comput. Chem.* **1989**, *10*, 982.
(27) Woo, T. K.; Cavallo, L.; Ziegler, T. *Theor. Chem. Acc.* **1998**, *100*, 307.
(28) Xu, Z.; Vanka, K.; Firman, T.; Michalak, A.; Zurek, E.; Zhu, C.; Ziegler, T. *Organometallics* **2002**, *21*, 2444.

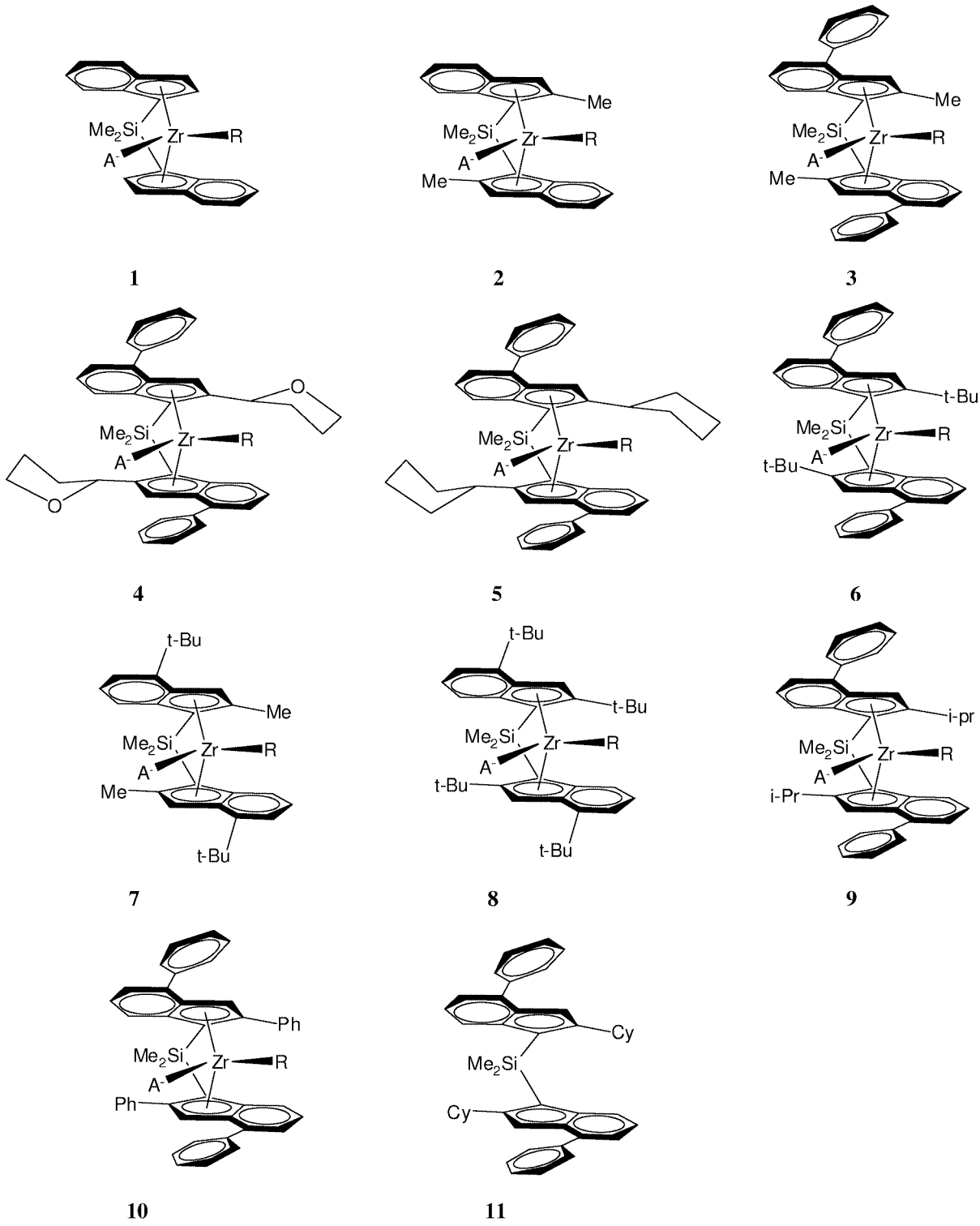

Figure 2. Structure of the catalyst systems under investigation. A^- and R represent the counterion $[MeB(C_6F_5)_3]^-$ and the growing chain, respectively.

and presented here for comparison.[13,29,30] The remaining catalysts listed in Figure 2 (catalysts **5**−**11**) have been designed by modifying substituents in the 2- and 4- positions of the indenyl ligand. Catalyst **4** has been designed by introducing THF in the 2-position of indenyl.[30] This motif has been made based on the notion that employing sterically demanding substituents in the 2-position can distort the β-hydrogen transfer transition-state geometry. Such a distortion raises the activation energy of termination by β-hydrogen transfer to monomer. This in turn increases the difference in the activation enthalpy between the termination and propagation steps, $\Delta\Delta H^{\ddagger}$, which leads to an increase in molecular weight. We used similar strategies to

(29) Spaleck, W.; Antberg, M.; Aulbach, M.; Bachmann, B.; Dolle, V.; Haftka S.; Küber, F.; Rormann, J.; Winter A. In *Ziegler Catalysts*; Fink G., Mülhaupt, R., Brintzinger., H.-H., Eds.; Springer-Verlag: Berlin, 1995; p 83.

(30) Yahata, T.; Ushioda, T.; Uwai, T.; Nakano, M. *Proceedings of The Global Business Forum, Polypropylene 2003, 12th Annual World Congress*; September 15−17; Zurich, Switzerland, 2003.

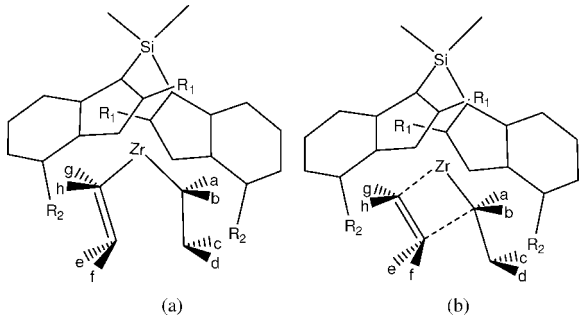

Figure 3. Structures of the α-agostic species (left) and the transition-state for olefin propagation (right).

develop the catalyst systems shown in Figure 2 (catalysts **5**−**11**). For example, **5** has been introduced by replacing THF with the cyclopentyl (Cyp) substituent which has similar steric bulk around the indenyl ligand. We extended our investigation to catalyst **11** which has the cyclohexyl (Cy), a bulkier ligand than Cyp, substituent in the 2- position. Furthermore, we considered a rigid phenyl substituent (catalyst **10**) to make a comparison with Cy which is a flexible ligand. Finally, a design was introduced which makes use of both electronic and steric effects by employing *t*-Bu. Thus, incorporating an electron donating substituent, *t*-Bu, in the 2- position of indenyl makes the Zr center more electron rich which prevents the counterion from making a stable contact ionpair.[31] Therefore, this makes insertion easier and consequently lowers the activation energy of the propagation step. In addition, introducing a sterically demanding substituent, *t*-Bu, in the 2- position of the indenyl ligand can distort the transition-state geometry of the termination step by β-hydrogen transfer to monomer. And this raises the activation energy of the termination step. Thus, catalysts **6** and **8** have been designed based on the strategy described above. We shall now discuss how the expectations described above are born out by calculations.

Chain Propagation. The chain propagation step is fundamental to polymerization and involves the binding of olefin to the metal center followed by insertion into the metal-alkyl bond. Olefin propagation follows the two most common routes known as 1,2-insertion (regio-regular) with the unsubstituted olefin carbon binding to the metal and 2,1-insertion (regio-error) with the unsubstituted olefin carbon binding to the α-carbon of the growing chain. Experimental[9] and theoretical[2] studies for early transition metal systems indicated that the 1,2-insertion is the most accessible route. Thus we shall only consider propagation following the 1,2-insertion.

The transition-state structures were optimized for all of the complexes for which we were able to calculate a barrier. A schematic representation of the transition-state structure is shown in Figure 3b. We examined the activation energy of the transition-state for the propagation step relative to the α-agostic species (π-complex) shown in Figure 3a. This species is a common intermediate for both propagation and chain transfer reaction pathways. For both model systems (EP and PP), the polymeryl chain was represented by C_4H_9 (**a** = H, **b** = H, **c** = Me and **d** = Me), while the nature of the approaching monomer unit was defined by **e**, **f**, **g**, and **h**. The structure in Figure 3a can be viewed as representing ethylene/propylene π-complexation following a propylene insertion. Thus, **c** = Me, **d** = Me, **e** = Me, and **f** = H for homopolymerization of propylene (PP) and **c** = Me, **d** = Me, **e** = H, and **f** = H for copolymerization of ethylene with propylene (EP).

Table 1. Activation Energies (kcal/mol) of Propagation and Chain Transfer to Monomer

	EP			PP		
cat.	$\Delta H^{\ddagger b}_{\beta\text{-H}}$	$\Delta H^{\ddagger c}_{\text{ins}}$	$\Delta\Delta H^{\ddagger d}$	$\Delta H^{\ddagger b}_{\beta\text{-H}}$	$\Delta H^{\ddagger c}_{\text{ins}}$	$\Delta\Delta H^{\ddagger d}$
1	4.6	1.8	2.8	9.1	4.0	5.1
2	6.3	2.1	4.2	9.4	3.7	5.7
3	7.4	2.4	5.0	11.7	4.0	7.7
4	5.0	no barrier[a]	>5.0	10.2	3.2	7.0
5	7.9	no barrier	>7.9	13.0	3.8	9.2
6	11.1	no barrier	>11.1	12.7	0.5	12.2
7	12.7	3.6	9.1	13.0	7.2	5.8
8	13.5	2.3	11.2	14.8	7.0	7.8
9	8.9	no barrier	>8.9	13.2	3.8	9.4
10	11.6	no barrier	>11.6	18.7	2.3	16.4
11	11.3	no barrier	>11.3	14.8	4.0	10.8

[a] It is a downhill process. [b] Barrier of termination relative to the α-agostic π-complex. [c] Barrier of insertion relative to the α-agostic π-complex. [d] $\Delta\Delta H^{\ddagger} = \Delta H^{\ddagger}_{\beta\text{-H}} - \Delta H^{\ddagger}_{\text{ins}}$.

Table 2. Relative Energies (kcal/mol) of All the Stationary Points of Catalyst 3

	$RC^{\pi}{}_{\alpha}{}^{a}$	$RC^{\pi}{}_{\beta}{}^{b}$	βH-TS[c]	βH-PC[d]	Ins-TS[e]	Ins-PC[f]
EP	0.0	0.7	7.4	−2.7	2.4	−15.3
PP	0.0	1.7	11.7	1.9	4.0	−5.7

[a] α-Agostic π-complex. [b] β-Agostic π-complex. [c] Barrier of termination relative to the α-agostic π-complex. [d] β-H transfer product complex. [e] Barrier of insertion relative to the α-agostic π-complex. [f] Insertion product complex.

The activation energies for the propagation step involving the two models PP and EP are collected in Table 1 for all of the systems shown in Figure 2. In all cases, the PP system representing propylene homopolymerization has a higher insertion barrier than the corresponding EP model system, which represents ethylene/propylene copolymerization. The observed energy difference between these two model systems arises from steric factors. The relative energies of all the stationary points of catalyst **3** are given in Table 2. The α-agostic complex is slightly more stable than the corresponding β-agostic complex for both EP and PP systems. Table 3 shows the possible interactions[32] involving the growing chain, the monomer, and the substituents on the ligand. As seen from the table, the PP system has at least one interaction type (α) which involves the polymeryl chain (**c** = Me) and the substituent **e** on the monomer (*e* = Me).

Table 3 also provides additional interactions, which take into account the substituents on the indenyl ligand (R_1 and R_2) and the two methyl substituents on the growing chain (**c** and **d**). The superscripts indicated for interaction types β, χ, δ, and ε reflect the difference in strength of an interaction for the various substituents considered in this study The interaction types indicated in Table 3 are defined below:

α: Interaction between the growing chain (*c* = Me) and the monomer (*e* = Me). This interaction is zero if a trans interaction exists between the growing chain and the 1,2-inserting polymer.

β: Interaction between the monomer (*e* = Me) and the substituents on the indenyl ligand (R_1).

χ: Interaction involving the growing chain (*d* = Me) and the substituent on the indenyl ligand (R_1).

(31) Chen, E.; , Y.-X.; Marks, T. J. *Chem. Rev.* **2000**, *100*, 1391.

(32) Froese, R. D. J. In *Computational Modeling for Homogeneous and Enzymatic Catalysis. A Knowledge-Base for Designing Efficient Catalysts*; Morokuma, K., Musaev, D. G., Eds.; WILEY-VCH Verlag GmbH & Co. KGaA: Weinheim, 2008; p 149.

Table 3. Possible Interactions Involving the Propagation and β-H Transfer Transition-States

		substituents										
cat.		a	b	c	d	e	f	g	h	R_1	R_2	interactions
1	EP	H	H	Me	Me	H	H	H	H	H	H	
	PP	H	H	Me	Me	Me	H	H	H	H	H	α
2	EP	H	H	Me	Me	H	H	H	H	Me	H	χ
	PP	H	H	Me	Me	Me	H	H	H	Me	H	$\alpha + \beta + \chi$
3	EP	H	H	Me	Me	H	H	H	H	Me	Ph	$\chi + \delta + \varepsilon$
	PP	H	H	Me	Me	Me	H	H	H	Me	Ph	$\alpha + \beta + \chi + \delta + \varepsilon$
4	EP	H	H	Me	Me	H	H	H	H	Cyp	Ph	$\chi^2 + \delta + \varepsilon$
	PP	H	H	Me	Me	Me	H	H	H	Cyp	Ph	$\alpha + \beta^2 + \chi^2 + \delta + \varepsilon$
5	EP	H	H	Me	Me	H	H	H	H	THF	Ph	$\chi^3 + \delta + \varepsilon$
	PP	H	H	Me	Me	Me	H	H	H	THF	Ph	$\alpha + \beta^3 + \chi^3 + \delta + \varepsilon$
6	EP	H	H	Me	Me	H	H	H	H	*t*-Bu	Ph	$\chi^4 + \delta + \varepsilon$
	PP	H	H	Me	Me	Me	H	H	H	*t*-Bu	Ph	$\alpha+\beta^4+\chi^4+\delta+\varepsilon$
7	EP	H	H	Me	Me	H	H	H	H	Me	*t*-Bu	$\chi + \delta^2 + \varepsilon^2$
	PP	H	H	Me	Me	Me	H	H	H	Me	*t*-Bu	$\alpha + \beta + \chi + \delta^2 + \varepsilon^2$
8	EP	H	H	Me	Me	H	H	H	H	*t*-Bu	*t*-Bu	$\chi^4 + \delta^2 + \varepsilon^2$
	PP	H	H	Me	Me	Me	H	H	H	*t*-Bu	*t*-Bu	$\alpha + \beta^4 + \chi^4 + \delta^2 + \varepsilon^2$
9	EP	H	H	Me	Me	H	H	H	H	*i*-Pr	Ph	$\chi^5 + \delta + \varepsilon$
	PP	H	H	Me	Me	Me	H	H	H	*i*-Pr	Ph	$\alpha + \beta^5 + \chi^5 + \delta + \varepsilon$
10	EP	H	H	Me	Me	H	H	H	H	Ph	Ph	$\chi^6 + \delta + \varepsilon$
	PP	H	H	Me	Me	Me	H	H	H	Ph	Ph	$\alpha + \beta^6 + \chi^6 + \delta + \varepsilon$
11	EP	H	H	Me	Me	H	H	H	H	Cy	Ph	$\chi^7 + \delta + \varepsilon$
	PP	H	H	Me	Me	Me	H	H	H	Cy	Ph	$\alpha + \beta^7 + \chi^7 + \delta + \varepsilon$

δ: Interaction involving the growing chain (d = Me) and the substituent on the indenyl ligand (R_2).

ε: Interaction involving the growing chain (c = Me) and the substituent on the indenyl ligand (R_2).

Since the EP and PP systems are represented by the same polymeryl chain, C_4H_9, these interaction types (χ, ε, and δ) are not able to explain the observed activation energy differences for the propagation step. However, these interactions are helpful in understanding why the β-H transfer transition-state activation barrier is higher than the corresponding propagation step. This will be discussed in the next section.

Overall, the more bulky substituents on position **e**, the higher the propagation barrier. And this explains why insertion of an ethylene monomer is preferred compared with insertion of a propylene monomer for all the catalyst systems considered in this investigation. For each model system, the magnitude of the insertion barrier is affected by the nature of the substituents on the ligand (R_1 and R_2).

Chain Transfer to Monomer. Chain transfer to monomer (β-H transfer) is the predominant termination pathway, and it is computationally simple to understand molecular weight control using this mechanism. As shown in Figure 4, the β-H transfer mechanism involves the transfer of a β-H from the polymeryl chain to the β-C of the monomer. For this reaction pathway, we observed a β-agostic intermediate (Figure 4, left) which involves the Zr atom and β-H of the polymeryl chain. A schematic representation of the transition-state structure is also shown in Figure 4 (right).

Figure 5 presents key optimized geometrical parameters of insertion and β-H transfer transition-states for propylene homopolymerization. Since the geometrical parameters are similar for each model system (EP and PP), catalyst **2** was used as a representative example.

For the EP system, the β-H transfer process involves the cleavage of a tertiary C−H bond and the formation of a primary C−H bond. A primary C−H bond is stronger than the tertiary C−H bond. Thus, the β-H transfer transition-state provides stabilization energy to compensate the energy required to break the tertiary C−H bond.[17] However, for the PP system, a tertiary bond is broken and a secondary bond is formed. As a consequence, PP has a higher barrier than EP since secondary C−H formation for PP is less stabilized in the β-H transfer transition state than primary C−H formation.[17] Thus, the differences in the barriers for the β-H transfer between the EP and PP systems are primarily electronic in origin. The energetics of the β-H transfer reaction activation energies for the various catalytic systems under investigation are given in Table 1. Similar to the propagation step, the β-H transfer activation energy for the PP system is higher than the EP system for all the catalyst systems considered in Figure 1. Furthermore, incorporation of a methyl substituent in position **e** destabilizes the β-H transfer transition state structure for the PP system. This destabilization occurs as a result of interactions between the two methyl substituents on **c** and **e** positions (Figure 3). There is also another interaction (β) between the methyl group on position **e** and the various substituents on the indenyl ligand (R_1). The most crucial interactions in the β-H transfer transition-state structure are the ones which involve the χ, ε and δ interaction types. In this case, the polymer chain is positioned in such a way that the geometrical layout of the transition-state cannot avoid the key interactions described above. This is not the case for the propagation transition-state. This explains why the activation barriers for the β-H transfer process are higher than the corresponding insertion barriers for both EP and PP systems. This has been observed for all the catalysts considered in this study.

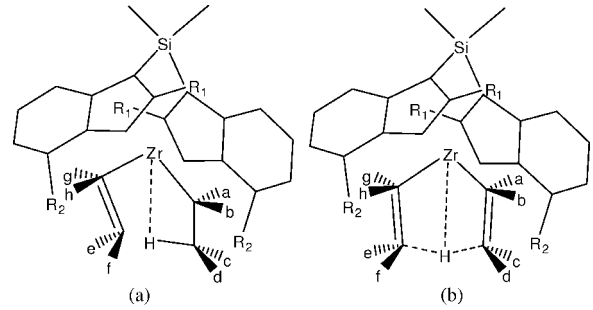

R_1 = H, Me, *i*-Pr, *t*-Bu, THF, Cyp, Cy, Ph; R_2 = Ph, *t*-Bu

Figure 4. Structures of the β-agostic species (left) and the transition-state for chain transfer to monomer (right).

The activation energies listed in Table 1 account for the influence of indenyl substitution pattern. For instance, the activation barriers for catalyst **1** which lacks indenyl substitution in the 2- and 4- positions are 4.6 and 9.1 kcal/mol for EP and PP systems, respectively. The incorporation of methyl in the 2-position (catalyst **2**) raises the barrier to 6.3 and 9.4 kcal/mol, respectively. And the $\Delta\Delta H^{\ddagger}$, which is a measure of molecular weight, increased to 4.2 and 5.7 kcal/mol for EP and PP models, respectively. Experimentally,[13] it has been found that this catalyst was the first example which led to the development of bisindenyl zirconocenes whose performance approaches that of industrial Ti-based catalysts. Combining substitution in the 2- and 4- positions (catalyst **3**) led to one of the most successful zirconocene catalysts for propylene homopolymerization.[13] Our calculations also demonstrated that **3** is a better catalyst than **1** and **2**. Overall, these results underline the importance of ligand steric effects in designing efficient catalysts for homo- and copolymerization.

Analysis of the activation barriers reported for catalysts **1**, **2**, and **3** along with the corresponding $\Delta\Delta H^{\ddagger}$ prompted us to undertake a detailed investigation of the indenyl liagnd substitution pattern. Thus, replacing the methyl group in position 2 of catalyst **3** with THF (five different binding modes were considered and the lowest energy structure is shown in Figure 2), leads to the development of **4.** Catalyst **4** is more active than **3** with a lower insertion barrier. We did not manage to

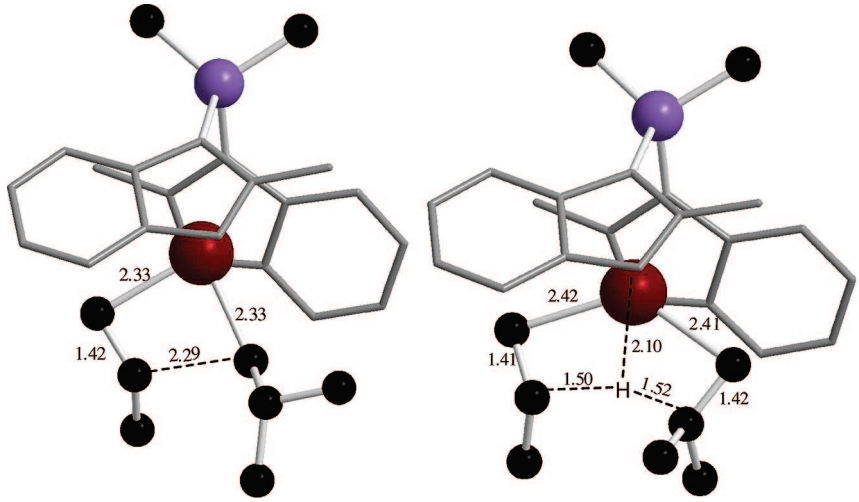

Figure 5. Optimized transition-state geometries (Å) of insertion (left) and β-H transfer reaction (right) for propylene homopolymerization. The counterion and hydrogen atoms are omitted for clarity.

locate the insertion transition-state for the EP system (downhill process). However, we believe this catalyst gives a higher molecular weight than **3** for ethyelene−propylene copolymerization (EP system). It is evident from the table that there is no significant difference between **3** and **4** toward propylene homopolymerization (PP). Incorporation of a cyclopentyl ligand in the same position, which has similar steric hindrance as THF, gives rise to catalyst **5**. This appears to be a promising catalyst toward homo- and copolymerizations. Careful analysis of the interaction types (χ, ε, and δ) led us to the development of **6** which bears a *t*-butyl group in the 2 position. The insertion barriers for both the EP and PP systems decrease significantly, whereas the β-H transfer activation barrier for the EP system increases significantly at the same time. Thus, the incorporation of a sterically demanding substituent in the 2-position increases the $\Delta\Delta H^{\ddagger}$ value. We observed a similar trend by incorporating a bulky substituent (*t*-Bu) in the 4-position. This underlies the importance of the three interaction types. It would appear that **6**, **8**, **10**, and **11** are the most promising catalysts toward homo- and copolymerization. Overall, our findings provide new insights into the development and design of C_2-symmetric catalysts for ethylene−propylene copolymerization. Furthermore, these results can be utilized in the development of other symmetric catalysts, such as the systems shown in (a)−(c) of Figure 1 (C_s and C_1). Therefore, it is noteworthy to consider electronic and steric factors for designing potential zirconocene catalysts toward homo- and copolymerization. We are currently in the process of investigating C_s and C_1 fluorenyl-based catalysts for ethylene and propylene copolymerization.

Conclusions

In summary, we have presented a quantum mechanical and molecular mechanics (QM/MM) investigation on eleven C_2-symmetric zirconocenes. We have thoroughly examined interactions involving the growing chain, the monomer and the substituents on the ligand. On this basis, we investigated five interaction types[32] denoted by α, β, χ, δ, and ε. An analysis of these interaction types led us to the development of new C_2-symmetric catalysts (see Figure 2) for homo- and copolymerizations. We have demonstrated computationally that incorporating sterically demanding substituents in the 2- and 4-positions can significantly increase molecular weight in copolymerization. In the current investigation, we have only considered one mechanism for chain termination, namely hydrogen transfer to monomer. Other mechanisms are possible. However, they all have considerably higher activation energies than propagation.[32] They are, as a consequence, not considered here, since they are unlikely to be the cause of the low molecular weight[17] afforded by some metallocenes in ethylene/propylene copolymerization.

Acknowledgment. We would like to thank Total for financial support. T.Z. thanks the Canadian government for a Canada Research Chair.

Supporting Information Available: Optimized Cartesian coordinates for all the stationary points. This material is available free of charge via the Internet at http://pubs.acs.org.

OM800731Y